"Ladder" structure in tonal noise generated by laminar flow around an airfoil

Tze Pei Chong
School of Engineering and Design, Brunel University, Uxbridge, UB8 3PH, United Kingdom
t.p.chong@brunel.ac.uk

Phillip Joseph
Institute of Sound and Vibration Research, University of Southampton, Southampton, SO17 1BJ, United Kingdom
pfj@isvr.soton.ac.uk

Abstract: The presence of a "ladder" structure in the airfoil tonal noise was discovered in the 1970s, but its mechanism hitherto remains a subject of continual investigation in the research community. Based on the measured noise results and some numerical analysis presented in this letter, the variations of four types of airfoil tonal noise frequencies with the flow velocity were analyzed individually. The ladder structure is proposed to be caused by the acoustic/hydrodynamic frequency lag between the scattering of the boundary layer instability noise and the discrete noise produced by an aeroacoustic feedback loop.

PACS numbers: 43.28.Ra, 43.28.Bj [VO]
Date Received: March 06, 2012 **Date Accepted:** March 28, 2012

1. Introduction

This letter is concerned with an experimental investigation into a unique "ladder" feature of the airfoil tonal noise. Figure 1(a) shows a typical spectrum of the noise radiated by an airfoil in a low Reynolds number laminar flow. The figure reveals a broad spectral hump centered on frequency, f_s, in addition to the presence of a number of discrete tones occurring at frequency f_n. The frequency of the tone of the highest sound pressure level is defined here to be the "dominant" frequency, $f_{n\text{-max}}$. Paterson *et al.*[1] have performed a systematic study on isolated airfoil noise in an anechoic environment. Based on calculations of the laminar boundary layer on a flat plate, they proposed the following empirical formula for the main tonal central frequency f_s:

$$f_s = 0.011\mathrm{U}^{1.5}/(Cv)^{0.5}, \tag{1}$$

where U is the velocity, C is the chord, and v is the kinematic viscosity of air. An assumption made in Eq. (1) is that f_s is independent of the airfoil angle of attack. Another key observation by Paterson *et al.*[1] is the existence of the so-called ladder structure for the dependence of tonal frequency on flow velocity. These two frequency dependencies are illustrated in Fig. 1(b), which indicates that over a small velocity range, the discrete frequency of the tone f_n, follows a power law of 0.8. As the velocity is increased, the dominant tonal frequency $f_{n\text{-max}}$ is observed to follow a smooth curve but then jumps to another parallel curve with the same $\mathrm{U}^{0.8}$ dependence. It appears that several frequency jumps can occur over the velocity range. The $\mathrm{U}^{1.5}$ dependency shown in Eq. (1) therefore represents the average frequency variation of the dominant tone.

Using the experimental results of Paterson *et al.*,[1] Tam[2] deduced the following modified frequency evolution law for the discrete tones, f_n:

$$f_n = 6.85n\mathrm{U}^{0.8}, \tag{2}$$

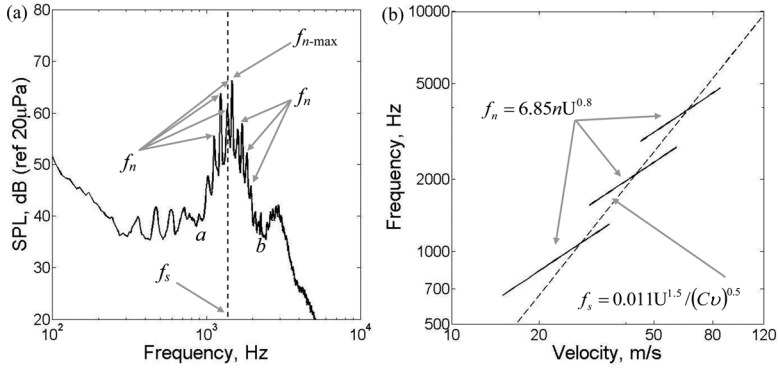

FIG. 1. (a) Illustrations of the f_s, main tonal frequency; f_n, discrete frequencies; and $f_{n\text{-max}}$, dominant discrete frequency, in a typical airfoil tonal noise spectrum. (b) Scaling law of f_s (– – –) based on the Paterson *et al.* (Ref. 1) formula [Eq. (1)]. The variations of f_n with velocity (—) can be described by the Tam (Ref. 2) formula [Eq. (2)]. The ladder structure is shown here.

where n is an integer. In an attempt to explain the presence of multiple tones in the spectrum Tam[2] proposed a self-excited feedback-loop concept and conjectured that hydrodynamic instabilities are shed into the downstream wake, which then becomes localized at some distances downstream of the trailing edge. Some of these wake instability modes are unstable where they radiate acoustic wave upstream and disturb the boundary layer near the trailing edge. A closed loop is then formed in which instability modes produce sound that then drives the instability mode, and so on. In Tam's model,[2] the nth tonal frequency occurs when the total phase change around the loop is equal to $2\pi n$. Whilst this phase condition may explain the existence of several distinct tones in the noise spectrum [e.g., Fig. 1(a)], it cannot explain the ladder structure observed in the noise data because the feedback loop model cannot predict the tone amplitudes.

Tam's feedback hypothesis was later modified by Arbey and Bataille.[3] They argued that the broadband component of the noise spectrum was due to diffraction and scattering of Tollmien–Schlichting (TS) waves at the trailing edge, whereas the discrete tone contributions are related to an alternative aeroacoustic feedback mechanism. In their model, discrete tone occurring at frequency f_n is due to a feedback loop between the boundary layer instabilities at the trailing edge and the upstream propagating acoustic wave that reinforces the point upstream of the trailing edge at which the instabilities originated. This modified acoustic feedback loop, however, remains incapable of explaining why the dominant tone frequencies $f_{n\text{-max}}$ tend to jump to other rungs as the flow velocity progresses. Based on the feedback model,[3] Kingan and Pearse[4] proposed a theoretical model to predict the discrete tone frequency (f_n) over the range of frequencies that satisfy integer values of n for which TS wave amplification occurs. In the paper they compare the frequency that corresponds to the maximum amplification of TS wave ($f_{\text{TS-max}}$) with the multidiscrete tone frequencies f_n over several flow velocities. They found that $f_{\text{TS-max}}$ and f_n scale in proportion to approximately $U^{1.5}$ and $U^{0.8}$, respectively. They then used the difference in the velocity scaling laws to explain the ladder structure. This conjecture has yet to be proven experimentally. In addition, the paper neither confirms the role of the central frequency of the tonal hump (f_s), nor clarifies the mechanism under which the dominant tone frequencies ($f_{n\text{-max}}$) are affected by the different velocity scaling laws. Other authors, such as McAlpine *et al.*[5] and Desquesnes *et al.*,[6] propose that the frequency of the dominant discrete tone ($f_{n\text{-max}}$), the frequency corresponding to the maximum amplification of the TS wave ($f_{\text{TS-max}}$) and the tonal hump frequency (f_s) tend to equal each other irrespective of the Reynolds number. The questions remain, however, about the physical implication of linking all these frequencies over a relatively large range of Reynolds numbers and their roles in the ladder structure.

The presence of an aeroacoustic feedback loop between the hydrodynamic instabilities and the radiated sound has been proven to play an essential role in the mechanism of airfoil tonal noise generation.[2–6] However, the precise details and nature of this loop and how it is related to the ladder structure have not been unequivocally established. A fundamental issue that remains to be addressed is the mechanism that creates the ladder structure of the airfoil tones with increasing flow velocity. This letter will study the tonal noise generated by laminar airfoil in the context of four frequency types—f_s, f_n, $f_{n\text{-max}}$, and $f_{\text{TS-max}}$—and discuss how they will vary with flow velocity.

2. Experiment setup

Airfoil noise measurements under free field conditions were made in the open jet wind tunnel at the University of Southampton, which is situated in an $8 \times 8 \times 8$ m anechoic chamber. The nozzle exit is of rectangular section with dimensions of 0.15×0.45 m. The turbulence intensity in the potential core is typically 0.1% at a Mach number of 0.3. The exit flow is also uniform (with less than 6% variation) in the spanwise direction inside the potential core. Background noise levels are very low and have been proven to be due to turbulent mixing in the jet. A more detailed description of this facility and its characteristics can be found in Chong *et al.*[7]

The airfoil under investigation here is an NACA0012 with a chord of 0.15 m and a span of 0.45 m. The airfoil has an aspect ratio of 3 to maintain a two-dimensional (2D) flow over most of its surface. The airfoil was held in the potential core by two side plates, which were attached to the nozzle lips. Following the wind tunnel correction scheme of Brooks *et al.*,[8] in this study an "effective" angle of attack (θ) of 1.4° was determined from a "geometrical" angle of 5°. The range of jet velocity under investigation here is from 25 to 50 m s^{-1}, corresponding to a range of Reynolds numbers, Re, of $2.5–5.0 \times 10^5$ based on the chord length. A microphone at polar angle of $\zeta = 90°$ and at 1.25 m from the airfoil trailing edge was used to measure the far field noise radiated from the airfoil. The microphone was mounted at the mid-span plane of the airfoil model. Noise data were sampled at 30 kHz for 13.33 s using a 24 bit analog-to-digital card. The digitized data were low-pass filtered at 15 kHz to avoid signal aliasing. The power spectra density of the noise was then obtained using a 4096 point fast Fourier transform and a Hamming window.

It is useful to note that the noise of the wind tunnel should not affect the feedback loop considered here. The existence of the loop itself needs to acoustically excite the origin of the boundary layer instability wave (on the airfoil surface) that sustains the noise source in the first place. Acoustical lock-on to other experimental facilities is unlikely as there is no hydrodynamic process present in the experiment to sustain such a loop, especially in an anechoic chamber. The boundary layers on both side-plates that hold the airfoil model will also be turbulent due to the sidewall boundary layer contamination effect. This is again unlikely to produce instability noise that might be able to generate extraneous feedback loops. The tonal hump and discrete tones frequencies (f_s, f_n, and $f_{n\text{-max}}$) measured in the present experiment are of the genuine values pertaining to a laminar airfoil.

3. Linear stability analysis

Linear stability analysis was undertaken of the boundary layer flow over the airfoil surface. Disturbances in the boundary layer are assumed to be spatially growing TS waves of frequency ω and slowly varying complex wave number ($\alpha = \alpha_r + i\alpha_i$). Following the method described by McAlpine *et al.*[5] and Kingan and Pearse,[4] the stream function $\psi(x, y)$ associated with the TS waves can be expressed in the form as

$$\psi(x,y) = \phi(y)\exp\left[i\left(\int \alpha(x)dx - \omega t\right)\right], \tag{3}$$

where (x, y) is a Cartesian coordinate system such that x is the streamwise direction and y is the wall-normal direction, ϕ is the perturbation amplitude, and t is time. The wave number of the least stable mode at any streamwise position x on the airfoil surface, though might be obtained by the propagation theory of Kim *et al.*,[9] has found to be adequately described by the classical Orr–Sommerfeld equation as

$$\phi^{(4)} - 2\alpha^2\phi^{(2)} + \alpha^4\phi = i\mathrm{Re}\left\{(\alpha U - \omega)\left(\phi^{(2)} - \alpha^2\phi\right) - \alpha U^{(2)}\phi\right\}, \tag{4}$$

where Re is the Reynolds number and U is the velocity profile at point x along the airfoil surface, and the superscripts on ϕ and U denote differentiation with respect to y.

In order to solve Eq. (4) to obtain the least stable modal wave numbers at a fixed (Re, ω) the velocity profile $U(y)$ must be known at a number of positions x along the airfoil surface. As boundary layer profiles were not measured in the present study, estimates of $U(y)$ were made using the public-domain code XFOIL in a similar approach to Kingan and Pearse.[4] In the present study, XFOIL was used to estimate the boundary layer shape factor at a number of positions along the chord of the pressure side of an NACA0012 airfoil, between the leading edge and the trailing edge in 2% chord intervals. As the pressure gradient on an airfoil varies along the chord, the Falkner–Skan velocity profile provides a suitable representation of the flow over the airfoil surface. Because each Falkner–Skan profile is associated with a unique shape factor, the velocity profile at each station that matches the predicted shape factor under consideration can be obtained.

Numerical solutions to the Orr–Sommerfeld equation of Eq. (4) were obtained using the Chebyshev matrix technique described by Kingan and Pearse.[4] The first point along the airfoil chord x_o at which an instability first appears is identified from the position at which $\mathrm{Im}\{\alpha_i\}$is less than 0. The amplification A of the TS wave, at any frequency, between x_o and near the trailing edge x_n is

$$A = \exp\left(-\int_{x_o}^{x_n} \alpha_i(x)dx\right). \tag{5}$$

4. Discussion of results

Figure 2(a) shows the distributions of the TS wave amplification A (at airfoil pressure side) as a function of frequency over velocity range of 22–40 ms^{-1} at $\theta = 1.4°$. Frequencies that correspond to the maximum level of amplification, identified as $f_{\mathrm{TS\text{-}max}}$, at each flow velocity are plotted in Fig. 2(b). $f_{\mathrm{TS\text{-}max}}$ is found to scale with $\mathrm{U}^{1.55}$.

The discrete tone frequency (f_n) over the range of frequencies for which TS wave amplification occurs can be predicted by[4]

$$F(f_n) \equiv \frac{1}{2\pi}\int_{x_o}^{x_n} \alpha_r(x)dx + \frac{f_n L}{c_o - \mathrm{U}_{\infty,L}} + \frac{1}{2} = n, \tag{6}$$

where $n = 1$, 2, 3, and so on. The first term on the right-hand side accounts for the phase change due to TS waves of wave number α_r convecting between x_o (first point of instability) to x_n (near the trailing edge). The second term accounts for the phase change due to the acoustic wave propagating between x_n back to x_o. Note that $L = (x_n - x_o)$, where c_o is the speed of sound and $\mathrm{U}_{\infty,L}$ is the average freestream velocity between x_o and x_n. The factor of 1/2 in Eq. (6) accounts for the 180° phase change due to the Kutta condition at the trailing edge.[3,4] The presence of the numerous discrete tones f_n in the measured noise spectra, such as those shown in Fig. 1(a), indicates that at a given velocity, $F(f_n)$ is satisfied for a wide range of n values. Each discrete frequency f_n thus corresponds to when the phase function $F(f_n)$ takes integer values n. Applying this argument to the airfoil, the discrete frequencies f_n satisfying Eq. (6) over

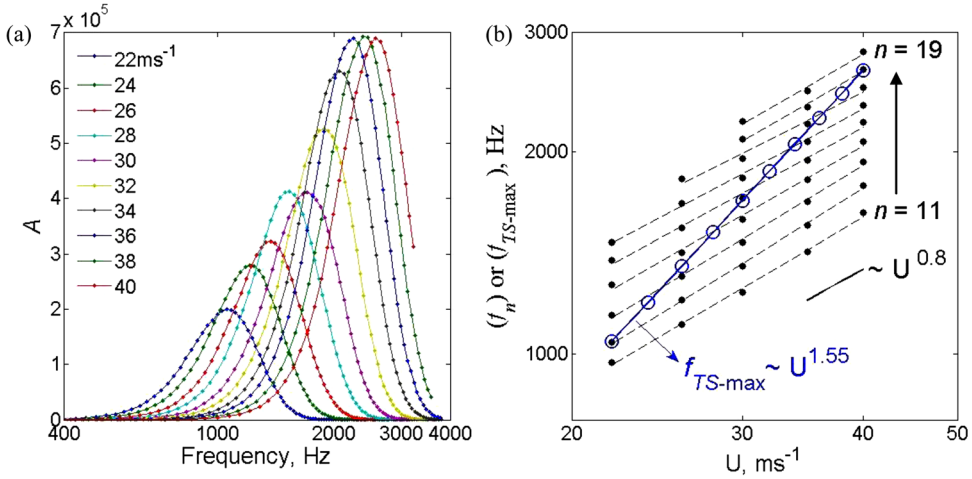

FIG. 2. (Color online) (a) Maximum TS waves amplification A (at airfoil pressure side) calculated for U = 22–40 ms^{-1} and at $\theta = 1.4°$. (b) Variations of the predicted f_n (--●--) for $n = 11$–19 and $f_{\text{TS-max}}$ (–○–) against U.

a range of velocities were calculated. The variations of $f_n(n = 11–19)$ with U computed from Eq. (6) are plotted in Fig. 2(b). The theoretical discrete frequencies f_n follow a velocity power law of approximately 0.8, similar to the value proposed by Tam.[2] Figure 2(b) also includes the frequencies of the most amplified instability waves $f_{\text{TS-max}}$ versus U, which clearly demonstrates that $f_{\text{TS-max}}$ can be best-fitted linearly with U, and it is not predicted to follow the classical ladder structure caused by the variation of the "rungs" of discrete tones f_n with U as shown in Fig. 1(b). However, $f_{\text{TS-max}}$ is predicted to follow closely the $U^{1.5}$ scaling law as observed by Paterson *et al.*[1] for the main tonal central frequency (f_s). This suggests a close physical relationship between the mechanisms producing the two frequencies. Moderately good agreement (about 10%–22% discrepancy) between the most amplified TS wave frequencies ($f_{\text{TS-max}}$) and the measured main tonal central frequencies (f_s) has been observed. Considering the level of approximations for the linear stability analysis, such an error is usually acceptable for

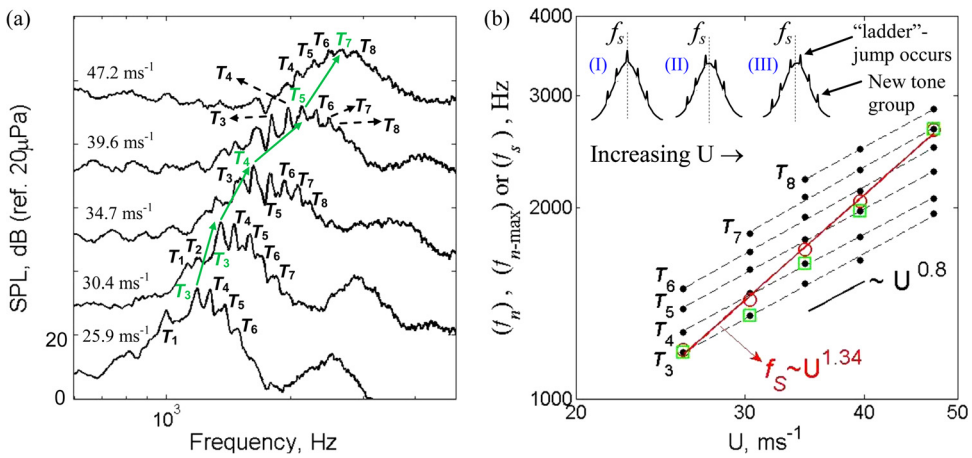

FIG. 3. (Color online) (a) Noise spectra (dB/Hz) presented at U = 25.9, 30.4, 34.7, 39.6, and 47.2 m s^{-1}. Each discrete tone frequency f_n at a particular U is represented by T_1, T_2, T_3, and so on, for the different tone groups. The sequence of the solid arrow lines (→) shows the variations of $f_{n\text{-max}}$ with respect to U. (b) Variations of the measured f_n (--●--) for T_3–T_8, f_S (–○–) and $f_{n\text{-max}}$ (□) against U. All the data presented here were determined from the spectra in (a).

TABLE 1. Summary of predicted and measured discrete tone frequencies at $U = 30.4\ m\ s^{-1}$ and $\theta = 1.4°$.

	Kingan and Pearse's $F(f)$ [Eq. (6)]	Present experimental result
f_n (Hz)		
$n = 12$	1351	1351
13	1468	1466
14	1585	1596
15	1705	1701
16	1828	1821

the prediction of the most amplified frequency. It is worth citing the results of McAlpine *et al.*,[5] which in one particular case the f_s was explicitly linked to the $f_{TS\text{-}max}$ where the error was 23%.

The results in Fig. 2(b) may provide an explanation for the mechanism of the ladder structure for laminar airfoils. The spectra shape pertaining to the tonal central frequency f_s, which features a broadband hump, has been linked in the past to that of the TS instability wave.[3] The TS wave is thus the main energy source that sustains the aeroacoustic feedback loop. At a particular value of U, the discrete frequencies f_n are produced by the resonant condition of the feedback loop but they must be contained within the lower and upper limits of the f_s envelope [indicated by a and b, respectively, in Fig. 1(a)]. In other words, f_n (for a particular n value), f_s, and $f_{TS\text{-}max}$ must all increase with velocity, *albeit at different rates*.

The characteristics of the ladder structure are now illustrated with the measured noise results in Figs. 3(a) and 3(b). Figure 3(a) shows the spectra of the airfoil noise at $U = 25.9$, 30.4, 34.7, 39.6, and $47.2\ m\ s^{-1}$. Note that each spectrum is increased by 20 dB relative to the spectrum at the next lower velocity in order to separate them on the figure. At the lowest velocity of $U = 25.9\ m\ s^{-1}$, feedback loop is expected to be present due to the existence of the multiple discrete tones f_n. Each discrete tone is labeled T_1, T_2, T_3, and so on. It is important to recognize that each tone component belongs to an n value associated with the feedback loop, as shown in Fig. 3(b). At $U = 25.9\ m\ s^{-1}$ the most dominant tone frequency $f_{n\text{-}max}$ of T_3 coincides with the peak of the broadband hump f_s. Other discrete tones f_n are also observed to occur around the broadband hump. At $U = 30.4\ m\ s^{-1}$, tone T_3 begins to lag in frequency relative to the peak of the broadband hump (f_s) due to its lower rate of change with velocity, but still maintains the largest amplitude at this particular flow velocity. However, at $U = 34.7\ m\ s^{-1}$, while T_3 lags further behind in frequency compared with the f_s, T_4 has now emerged as the particular tone component that is closest to the broadband hump peak. At this instant T_4 has replaced T_3 as the new dominant tone component and a ladder jump has occurred. Another ladder jump also occurs at $U = 39.6\ m\ s^{-1}$ from which T_5 becomes the most dominant tone component. As U further increases to $47.2\ m\ s^{-1}$, the most dominant tone frequency $f_{n\text{-}max}$ jumps to a new tone component of T_7.

Each clearly identifiable discrete tone frequency f_n obtained from the experiments is tabulated in Table 1 for the $U = 30.4\ m\ s^{-1}$ case. f_n predicted from Eq. (6) are also included in Table 1 for comparison. Excellent agreement is observed for the five tone frequencies deduced from the experiment with the prediction from $n = 12$ to 16. The average frequency spacing, Δf between adjacent tones obtained both in the experiment and prediction is about 118–120 Hz.

5. Conclusion

The most dominant instability tone frequency $f_{n\text{-}max}$ and its variation with velocity have been investigated experimentally, in which a classical ladder structure was produced. An aeroacoustic feedback loop alone cannot explain the existence of the ladder structure because it only explains the discrete tone frequencies f_n but not their amplitudes. Some

authors have attempted to link the most dominant tone frequency ($f_{n\text{-max}}$)with the frequency of the maximum amplification of the TS waves ($f_{\text{TS-max}}$).[5,6] Since the ladder structure is originated from the variations of $f_{n\text{-max}}$ with U, one would expect $f_{\text{TS-max}}$ to also exhibit the ladder structure in the spectrum. We have studied the variation of $f_{\text{TS-max}}$ at the airfoil's pressure side with flow velocity by solving the Orr–Sommerfeld equation. When the results are plotted in a log–log diagram in Fig. 2(b), no ladder structure is observed. However, these frequencies can be best fitted linearly and they follow the $U^{1.5}$ scaling law closely, which agrees very well with Paterson *et al.*[1] for the peak frequency of the broadband hump (f_s). This means that it is more meaningful to relate $f_{\text{TS-max}}$ with f_s. On the other hand, we have also found that each discrete tone f_n follows closely the $U^{0.8}$ scaling law, in conjunction with Tam's correlation.[2]

This difference in scaling laws thus suggests that the ladder structure is caused by the *frequency lag* between the maximum TS amplification (proportional to $U^{1.5}$, which eventually produces the broadband hump) and the multiple discrete tones [proportional to $U^{0.8}$, which is produced by an aeroacoustic feedback model explained in Eq. (6)]. The energy source for sustaining the aeroacoustic feedback loop comes from the TS waves. Therefore, the discrete tones should always embed within the frequency band of the broadband hump. It is important to note that the ladder jumping will therefore always be contained within the frequency band of the broadband hump.

The following summary can be described with the three illustrations (I), (II), and (III) shown in Fig. 3(b). When an airfoil is at a small angle of attack and the flow velocity is just sufficient to initiate tonal noise, the multiple discrete tones will occur around the symmetry of the frequency at f_s as depicted in (I). It is postulated that at this initial stage $f_{n\text{-max}} \approx f_s$ [e.g., see the $U = 25.9\,\text{m s}^{-1}$ case in Figs. 3(a) and 3(b)]. As illustrated in (II), when the flow velocity increases, f_s increases at a faster rate than any of the discrete tones. At some points in (III), a new tonal mode will eventually replace the previous most dominant tone (at lower frequency) to coincide with the peak of the broadband hump [e.g., see the $U = 34.7\,\text{m s}^{-1}$ case in Figs. 3(a) and 3(b)]. This is also the instance when a jump in frequency occurs as part of the ladder. This process will be repeated when the flow velocity is increased further until several ladder jumps occur, and be terminated when transition begins to occur near the trailing edge of the airfoil's pressure side at a sufficiently high Reynolds number.

Acknowledgments

This work is supported by DTI under the MSTTAR DARP program. The authors would like to thank Dr. Michael Kingan for allowing us use of his code for solving the Orr–Sommerfeld equation.

References and links

[1]R. Paterson, P. Vogt, M. Fink, and C. Munch, "Vortex noise of isolated airfoils," J. Aircr. **10**, 296–302 (1973).
[2]C. K. W. Tam, "Discrete tones of isolated airfoils," J. Acoust. Soc. Am. **55**, 1173–1177 (1974).
[3]H. Arbey and J. Bataille, "Noise generated by airfoil profiles placed in a uniform laminar flow," J. Fluid Mech. **134**, 33–47 (1983).
[4]M. J. Kingan and J. R. Pearse, "Laminar boundary layer instability noise produced by an aerofoil," J. Sound Vib. **322**, 808–828 (2009).
[5]A. McAlpine, E. C. Nash and M. V. Lowson, "On the generation of discrete frequency tones by the flow around an aerofoil," J. Sound Vib. **222**, 753–779 (1999).
[6]G. Desquesnes, M. Terracol, and P. Sagaut, "Numerical investigation of the tone noise mechanism over laminar airfoils," J. Fluid Mech. **591**, 155–182 (2007).
[7]T. P. Chong, P. F. Joseph, and P. O. A. L. Davies, "Design and performance of an open jet wind tunnel for aero-acoustic measurement," Appl. Acoust. **70**, 605–614 (2009).
[8]T. F. Brooks, D. S. Pope, and M. A. Marcolini, "Airfoil self-noise and prediction," NASA Reference Publication No. 1218 (1989).
[9]M. C. Kim, C. K. Choi, and D. Y. Yoon. "The onset of Görtler vortices in laminar boundary layer flow over a slightly concave wall," Eur. J. Mech. B/Fluids **29**, 407–414 (2010).